

THE PECULIAR VELOCITY FIELD IN THE PERSEUS-PISCES SUPERCLUSTER¹

JEFFREY A. WILLYCK

Space Sciences Laboratory and Department of Physics, University of California at Berkeley

Received 1989 September 26; accepted 1989 December 7

ABSTRACT

I describe the main results of a program to study peculiar motions of galaxies in the Perseus-Pisces supercluster. The data set consists of newly obtained CCD photometry and published 21 cm line widths for 320 spiral galaxies in the Perseus-Pisces region. The peculiar velocities of these objects are estimated using the Tully-Fisher relation, which has been calibrated with respect to an independent sample of cluster galaxies. Analysis of the Tully-Fisher data shows that the principal feature of the velocity field in the Perseus-Pisces region is a coherent streaming toward the Local Group. Nearly all the galaxies well in the foreground ($cz \lesssim 2000 \text{ km s}^{-1}$) have negative peculiar velocities of amplitude $\sim 1000 \text{ km s}^{-1}$. A great majority of objects in the background of the supercluster, out to redshifts of $\sim 7000 \text{ km s}^{-1}$, also have very large negative peculiar velocities. The supercluster ridge itself, at a redshift of $\sim 5000 \text{ km s}^{-1}$, appears to consist of positive and negative peculiar velocity groups of galaxies, but with negative peculiar velocities predominating both in amplitude and in number of objects involved; the net effect is a peculiar velocity of $\sim -450 \text{ km s}^{-1}$. The data for galaxies with the highest redshifts included in the sample, $cz \gtrsim 8000 \text{ km s}^{-1}$, are consistent with their being at rest.

These streaming motions in Perseus-Pisces are similar in amplitude and direction to those of elliptical galaxies in the southern sky, which have large positive peculiar velocities to distances of at least 4000 km s^{-1} . These have been modeled as arising from the pull of a "great attractor." If, as seems probable, the flow traced by the Perseus-Pisces spirals is physically related to that of the elliptical galaxies, the coherence length for this streaming motion is of order $100h^{-1} \text{ Mpc}$. It is unlikely that coherent motion on this scale can arise entirely from the great attractor; rather, it may be due in part to low-amplitude density fluctuations on much larger scales.

Subject headings: cosmology — galaxies: photometry — galaxies: redshifts

I. INTRODUCTION

Recent studies of the peculiar motions of galaxies (Dressler *et al.* 1987) have produced the unexpected result that the peculiar velocity field has a large amplitude and coherence length. This conclusion is based primarily on the observation that elliptical galaxies in the direction of the Hydra-Centaurus supercluster in the southern sky have large, positive peculiar velocities, out to distances of at least $\sim 4000 \text{ km s}^{-1}$. These motions have been modeled as arising from the pull of a "great attractor" (GA), a huge concentration of galaxies of mass $\sim 5 \times 10^{16} M_{\odot}$ (Lynden-Bell *et al.* 1988.) Faber and Burstein (1988) have shown that the elliptical galaxy data are best fitted by a model in which the mass concentration lies at a distance of 4200 km s^{-1} , in the direction $l = 309^{\circ}$, $b = 18^{\circ}$. In this model the GA induces a streaming motion which has an amplitude 535 km s^{-1} at the position of the Local Group and falls off roughly as $R^{-1.7}$ at greater distances.

To date, the peculiar velocity field well beyond the Local Supercluster, on the opposite side of the sky from the GA, has not been extensively probed. This region, centered on $l \sim 120^{\circ}$, $b \sim -30^{\circ}$, is dominated by the Perseus-Pisces (PP) supercluster, a massive, filamentary structure concentrated at a redshift of about 5000 km s^{-1} (Haynes and Giovanelli 1988.) There are relatively few ellipticals in the supercluster, so the flow studied by Lynden-Bell *et al.* is not well constrained there. The region is rich in late-type galaxies, however, and so is amenable to study via the Tully-Fisher relation (TF), the

luminosity-rotation velocity correlation for spirals. A large body of 21 cm data, including redshifts and line widths, has recently been made available for the PP region through the work of Giovanelli, Haynes, and coworkers (Giovanelli and Haynes 1985 and Giovanelli *et al.* 1986, hereafter, collectively, GH.) Photometric data provide the remaining element needed for application of the TF. In this *Letter*, I report the first results derived from a program of CCD photometry of PP spirals, undertaken with the aim of studying the velocity field in the supercluster region. These results are a condensation of more than 2 years' observations and data reduction, and their description is considerably abbreviated. A series of longer papers, to appear during the next year, will present data and describe details of the analysis which are sketched out here. In § II, I briefly describe the observations and data reduction, and in § III the calibration of the TF; in §§ IV and V, I present the basic evidence for large-scale inflow of the Perseus-Pisces galaxies; in § VI, I discuss the main results and their interpretation.

II. OBSERVATIONS AND DATA REDUCTION

The observations for this project were carried out at the Lick Observatory 1 m Nickel telescope during the period 1987 April through 1988 September. All the data used were obtained during photometric conditions. The raw data consist of images recorded on a Texas Instruments 500×500 CCD through a red filter. The effective wavelength of this system is $\sim 6700 \text{ \AA}$, with a bandwidth of $\sim 1200 \text{ \AA}$. Surface photometry was performed on each galaxy image, using an algorithm which approximates the isophotes of the galaxy as a series of concen-

¹ Based in part on observations made at Lick Observatory.

trick ellipses (Djorgovski 1985.) The ellipses fitted to the outer, disk-dominated portions of the galaxies provide an accurate measure of the axial ratios, used in estimating inclinations (Pierce and Tully 1988.) In addition, these asymptotic ellipses defined the aperture within which integral photometry was done. An exponential curve, fitted to the surface brightness profile of the disk, yielded an estimate of the additional luminosity which would be measured if the photometry could be carried out to arbitrarily large radii; this increment (typically ~ 0.05 mag) was then added to the luminosity measured directly in the outermost aperture, giving the "total" magnitude of each galaxy.

The resulting apparent magnitudes were subjected to three significant corrections prior to carrying out the Tully-Fisher analysis. First, a correction for internal extinction was done, using the formula given by Bothun *et al.* (1985); a factor of 0.6 was used as the ratio of R band to blue extinction. Second, the magnitudes were corrected for Galactic absorption. For this the blue extinctions (again multiplied by a factor of 0.6) given by Burstein and Heiles (1984) were used, for galaxies in the UGC catalog (Nilson 1973); for the few non-UGC galaxies, the average Burstein-Heiles extinctions of neighboring UGC galaxies were used. Finally, the magnitudes were K -corrected, using the prescription outlined by Schneider, Gunn, and Hoessel (1983), which is appropriate for magnitudes obtained from photon counting (as opposed to energy-flux measuring) detectors.

III. THE TULLY-FISHER CALIBRATION

In a crude sense, one estimates the peculiar velocity of a galaxy by $v_{\text{pec}} = H_0 d - v_r$, where d is the redshift-independent distance estimate, v_r is the observed redshift velocity (expressed in the microwave background rest frame), and H_0 is the Hubble constant. In practice, one can circumvent the need to obtain absolute galaxy distances (and thus an absolute value of H_0) by choosing an object (e.g., a galaxy cluster) with respect to which all distances are referenced. One then needs to determine the shape of the distance-indicator relation and to fix its zero point using the reference object. The distances relative to this standard of a set of independent objects may then be computed. For each of these a velocity-distance ratio may be calculated; a suitable averaging of these ratios then yields a *Hubble ratio*, i.e., a measure of the expansion rate of the universe in units of (velocity)/(distance relative to the reference object).

To accomplish this, I obtained CCD photometry for a large subset (125 galaxies) of the well-known 10 cluster sample of Aaronson *et al.* (1986, hereafter A86). Briefly, the calibration proceeded as follows: The TF was assumed to be of the form

$$M(\eta) = A - b\eta + c\eta^2, \quad (1)$$

where $M(\eta)$ is the expected value of the absolute magnitude of a galaxy with rotation velocity v_{rot} , and $\eta = \log(v_{\text{rot}}) - 2.5$ is a convenient measure of that velocity. For galaxies in the cluster sample, v_{rot} was inferred from the width of the 21 cm line measured at the 20% level as given by A86, corrected for redshift and inclination. Inclinations derived from the CCD surface photometry described above were used in favor of those given in A86. The absolute magnitudes in the above equation were defined as the apparent magnitudes at the distance of the reference object, which was taken to be the Coma Cluster. The expected apparent magnitude of an object at distance d is then given by $m = M + \mu$, where M is its TF-predicted absolute magnitude (eq. [1]), and $\mu \equiv 5 \log(d/d_{\text{Coma}})$

is its distance modulus. With this convention, equation (1) was fitted simultaneously to the R band total magnitudes and H I line widths in the 10 clusters; the free parameters were the constants A , b , and c characterizing the TF and the distance moduli of nine clusters (evidently, the distance modulus of Coma in this convention is zero.) The fit yielded the results $A = 14.89$, $b = 7.35$, $c = 3.35$, and an rms scatter of $\sigma = 0.30$ mag for the TF. The overall rms difference between individual galaxy distance moduli derived from the R band CCD TF, as compared with those derived from the H band TF of A86, was 0.27 mag, after the latter were adjusted for inclination differences. This value is very close to the H band TF scatter (~ 0.4 mag) and the R band TF scatter (0.3 mag) subtracted in quadrature, indicating that the two sets of TF moduli are in agreement to within the errors; a more detailed comparison will be presented in a future paper.

The cluster distance moduli obtained from the R band TF permitted an estimate of the Hubble ratio \mathcal{H} . Only the seven clusters with redshifts greater than 6000 km s^{-1} were used for this purpose, since peculiar velocities of several hundred km s^{-1} (which now appear common) can significantly distort the Hubble ratios of lower redshift clusters. A weighting scheme was employed to account for the various errors which affect the Hubble ratios, including the aforementioned peculiar velocities. This procedure led to the result $\mathcal{H} = 7550 \text{ km s}^{-1} d_{\text{Coma}}^{-1}$, with a 1σ error of $245 \text{ km s}^{-1} d_{\text{Coma}}^{-1}$, or about 3%.

Some consideration was given to possible biases associated with the cluster magnitude limits. As has been discussed by Terrikorpi (1987), the apparent magnitudes are biased toward brighter values than would be expected, at a given line width, in the absence of a magnitude limit. The size of this bias is about $(2/\pi)^{1/2} \sigma \sim 0.24$ mag for galaxies whose unbiased expected apparent magnitude is equal to the limiting magnitude for the given cluster and drops rapidly for brighter objects (Terrikorpi 1987.) In the cluster sample used here, a wide range of line widths was included in each cluster; therefore, only the lowest line width (faintest) galaxies in each cluster are significantly affected by this bias. A reasonable estimate of the size of the bias is that the distance modulus of any given cluster is affected by the largest value any single galaxy is likely to be affected, ~ 0.24 mag, divided by the number of objects per cluster. Since in general there are more than 10 objects per cluster, this amount is of order a few hundredths of a magnitude, corresponding to 1%–2% in distance. This is too small to affect the principal results presented in this *Letter*; moreover, a rigorous correction for the bias is complicated by the significant differences between the photographic magnitudes on which the sample selection was based and the R band CCD magnitudes used in the TF calibration. For these reasons, I have chosen to neglect this effect in the preliminary analysis presented here.

IV. PECULIAR VELOCITIES IN PERSEUS-PISCES

The Perseus-Pisces galaxy sample described here includes 274 galaxies with quality 21 cm profiles from GH, spanning the right ascension range $21^{\text{h}}40^{\text{m}}-4^{\text{h}}$ and the declination range $21^{\circ}5'-33^{\circ}5'$, as well as 46 galaxies in the $33^{\circ}5'-39^{\circ}5'$ declination zone, with 21 cm data kindly provided in advance of publication by M. Haynes. All galaxies in the sample have inclinations greater than 45° . The basic data set for the study of the velocity field consists of apparent magnitudes and 21 cm line widths, redshifts expressed in the microwave background rest frame, and positions on the sky. (The 21 cm line widths of GH

are defined somewhat differently from those of A86. Using a sample of 58 objects having line widths in both A86 and GH, I derived a transformation which adequately converts the GH line widths to the equivalent 20% widths used in A86. This transformation was applied to all objects in the PP sample prior to the analysis discussed below.) Peculiar velocities may be estimated from this data as follows. A distance modulus corresponding to Hubble flow is $\mu_{\text{Hub}} = 5 \log(v_r/\mathcal{H})$, where v_r is the observed radial velocity and \mathcal{H} is the Hubble ratio as computed from the cluster sample. A second distance modulus estimate may be formed from the TF information: $\mu_{\text{TF}} = m - M_{\text{TF}}$, where m is the observed apparent magnitude and M_{TF} is the absolute magnitude estimated from equation (1). The quantity $v_p = v_r(1 - 10^{0.2(\mu_{\text{TF}} - \mu_{\text{Hub}})})$ is then an estimate of the peculiar velocity. Because of the TF scatter, this estimate carries a statistical error $\sim 0.46\sigma v_r$, or about 14% of the redshift for $\sigma = 0.3$ mag.

In Figure 1, v_p is plotted as a function of observed redshift for galaxies in the Perseus-Pisces sample. (It is important to note that Fig. 1 does not plot v_p as a function of the distance inferred by the TF. This distance, as has been shown by a number of workers (see, e.g., Lynden-Bell *et al.* 1988), is strongly biased, particularly in the presence of density inhomogeneities. The redshift velocity itself is not strongly biased by line-of-sight density variations, and the peculiar velocity expressed at fixed redshift similarly avoids strong biases.) Also plotted are dashed lines corresponding to $v_p = 0.14v_r$, $v_p = 0$, and $v_p = -0.14v_r$, so that the effect of the TF scatter may be easily gauged. Several key features of this graph are apparent. First, of the eight objects with redshifts less than 2500 km s^{-1} , seven have peculiar velocities of $\sim -1000 \text{ km s}^{-1}$. Although few in number (the inevitable result of the large void in the foreground of the PP), these velocities are highly significant in view of the small error at low redshift. A second key feature of Figure 1 is the predominance of negative peculiar velocities in the densest regions of the PP supercluster. In the redshift range $3800 \leq cz \leq 6000 \text{ km s}^{-1}$, median value of v_p is -441 km s^{-1}

for 204 galaxies; the expected random deviation due to the TF scatter at these redshifts is $\sim 0.14(5000)/(204)^{1/2} = 49 \text{ km s}^{-1}$. In the range $6000 < cz \leq 7000 \text{ km s}^{-1}$ the median value of v_p is -839 km s^{-1} for 44 galaxies, as compared with an uncertainty of $\sim 0.14(6500)/(44)^{1/2} = 137 \text{ km s}^{-1}$. Both the supercluster ridge and its immediate background, then, have highly significant negative peculiar velocities. A third important aspect of Figure 1 is the absence of significant peculiar velocities at the highest redshifts in the sample. The median peculiar velocity for the 16 objects with $cz \geq 7800 \text{ km s}^{-1}$ is 358 km s^{-1} , as compared to an expected random scatter of $\sim 0.14(9000)/4 \simeq 315 \text{ km s}^{-1}$. Thus, the significant peculiar velocities which prevail in the supercluster are not detected at redshifts $\gtrsim 8000 \text{ km s}^{-1}$. The fact that the high-redshift objects in the PP sample do not continue to show negative peculiar velocities also argues that the Hubble ratio estimated from the cluster sample is essentially correct. If the negative peculiar velocities in the supercluster ridge were artifacts of an erroneous Hubble ratio, these velocities would persist, and indeed would be larger, at higher redshifts.

V. A GROUP IDENTIFICATION ANALYSIS

Figure 1 shows clearly the preponderance of negative peculiar velocities in the redshift range characteristic of the Perseus-Pisces supercluster. However, it contains all the noise inherent in distance estimates obtained via the TF; one would like somehow to get a "smoother" picture of the velocity field. One way to do this is to identify groups of galaxies, suitably average the apparent peculiar velocities of the individual members, and obtain a less noisy "group velocity." I have done this by using proximity in redshift space as the basic criterion for placing galaxies in groups; specifically, group members must have radial velocities within about 250 km s^{-1} of a mean value, while the velocity equivalent of their angular separations must be smaller than $\sim 500 \text{ km s}^{-1}$. The Tully-Fisher information is used only very conservatively in the grouping process, for the purpose of distinguishing groups which overlap in redshift

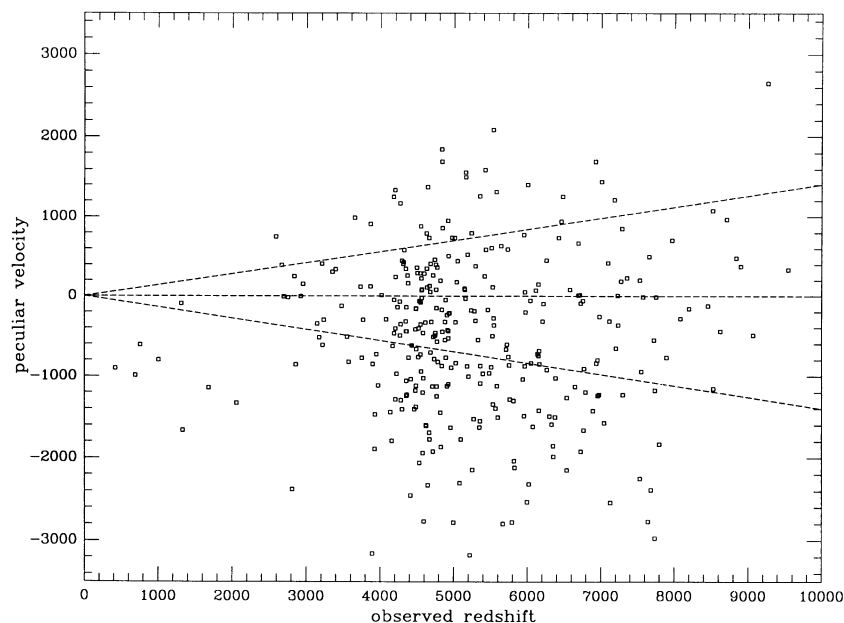


FIG. 1.—Peculiar velocities inferred from the Tully-Fisher relation plotted as a function of redshift, for galaxies in the Perseus-Pisces sample. The diagonal dashed lines represent the 1σ errors for these velocities, which result from a TF scatter of 0.3 mag.

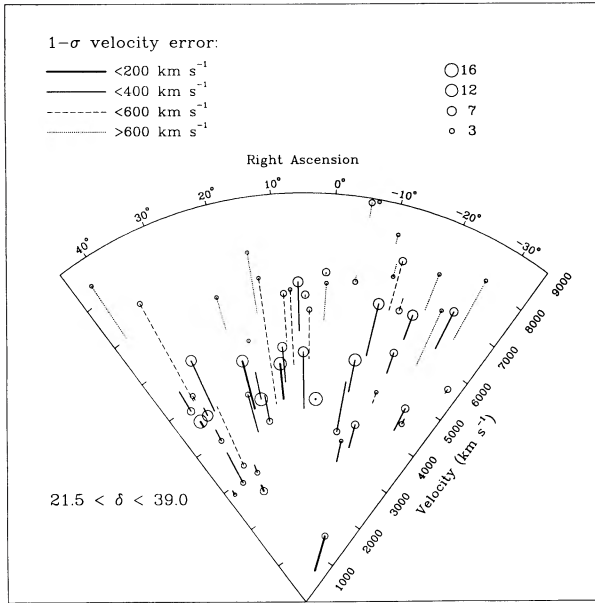


FIG. 2.—Positions and peculiar velocities of groups identified as described in § V. The velocity vectors end on the median redshift of the groups, which have typical velocity dispersions $\lesssim 250 \text{ km s}^{-1}$; the positions of the ends of these vectors therefore carry little uncertainty. The length of the vectors, and therefore also the positions (*open circles*) of the groups, carry uncertainty associated with the scatter of the Tully-Fisher relation. This uncertainty (1σ value) is coded by the line type of the velocity vector, as described by the key in the upper left of the figure. The number of objects in each group is coded by the size of the open circle, as described by the key in the upper right of the figure.

space but which, plausibly, are widely separated in physical space. Requiring grouped objects to have very similar radial velocities minimizes the effects of biased distances discussed briefly in the previous section.

When the grouping algorithm was applied to the PP sample, 280 galaxies were assigned to 56 groups. The inferred positions and peculiar velocities of these groups are shown in Figure 2. The velocity field around Perseus-Pisces suggested by Figure 2 is complex and is not describable simply in terms of a large-scale flow. There are a number of substantial groups in the supercluster ridge whose inferred peculiar velocities are consistent with their being at rest, and others with clearly detected positive peculiar velocities. However, most of the more populous groups are falling into the PP ridge from the background

with negative peculiar velocities of amplitude $\sim 1000 \text{ km s}^{-1}$. The large-scale streaming motion thus manifests itself in the predominance, but not exclusivity, of negative peculiar velocities. Smaller scale motions, most likely due to the pull of the PP filament and the push of the foreground void, are superposed on the large-scale flow and can either reinforce it (generally in the background of the supercluster) or work against it (in the foreground.) This fact makes a quantitative study of the flow quite difficult; future analyses must separate the component of the motion associated with very large scale streaming from that associated with the highly visible density inhomogeneities in Perseus-Pisces.

VI. DISCUSSION

The results I have presented here reinforce a growing body of evidence suggesting that the peculiar velocity field in the nearby universe possesses a very large coherence length. The motion which has been modeled by the flow toward a great attractor is in the same general direction, and on the opposite side of the sky, as the overall motion of galaxies in Perseus-Pisces depicted in Figure 2. Since the GA flow is clearly detected out $\sim 4000 \text{ km s}^{-1}$ in the southern sky, while the PP flow extends to $\sim 7000 \text{ km s}^{-1}$ in the north, the coherence scale for the combined samples is on the order of $100h^{-1} \text{ Mpc}$. In the model of Faber and Burstein (1988), the amplitude of the large-scale streaming induced by the GA at the position of the main PP ridge is $\sim 160 \text{ km s}^{-1}$. It is unlikely that the observed velocity of the ridge, $\sim 450 \text{ km s}^{-1}$, can be accounted for by the GA model alone. It is possible that the coherent streaming motions probed by both the ellipticals and the PP spirals arise in part from low-amplitude, very large scale density fluctuations not clearly seen in redshift surveys carried out to date. Density fluctuations at the 5%–10% level, on scales $\gtrsim 100h^{-1} \text{ Mpc}$, might account for the observed streaming motions, at least in a fairly high density ($\Omega \simeq 1$) universe. Dramatic objects such as the GA and Perseus-Pisces would then be responsible for smaller scale motions which are superposed on the large-scale flow.

I am grateful to Stuart Bowyer, Michael Strauss, Marc Davis, Sandy Faber, and Stephane Courteau for helpful discussions. In addition, I would like to thank Martha Haynes for providing me with H I data in advance of publication. The suggestions of the anonymous referee helped significantly improve the final draft of the *Letter*. This work was partially supported by NASA contract NAS8-32577.

REFERENCES

- Aaronson, M., Bothun, G., Mould, J., Huchra, J., Schommer, R. A., and Cornell, M. E. 1986, *Ap. J.*, **302**, 536 (A86).
 Bothun, G. D., et al. 1985, *Ap. J. Suppl.*, **57**, 423.
 Burstein, D., and Heiles, C. 1984, *Ap. J. Suppl.*, **54**, 33.
 Djorgovski, S. 1985, Ph.D. thesis, University of California at Berkeley.
 Dressler, A., Faber, S. M., Burstein, D., Davies, R. L., Lynden-Bell, D., Terlevich, R. J., and Wegner, G. 1987, *Ap. J. (Letters)*, **313**, L37.
 Faber, S. M., and Burstein, D. 1988, in *Large-Scale Motions in the Universe: A Vatican Study Week*, ed. V. C. Rubin and G. V. Coyne (Princeton: Princeton University Press), p. 115.
 Giovanelli, R., and Haynes, M. P. 1985, *A. J.*, **90**, 2445.
 Giovanelli, R., Haynes, M. P., Myers, S. T., and Roth, J. 1986, *A. J.*, **92**, 250.
 Haynes, M. P., and Giovanelli, R. 1988, in *Large-Scale Motions in the Universe: A Vatican Study Week*, ed. V. C. Rubin and G. V. Coyne (Princeton: Princeton University Press), p. 31.
 Lynden-Bell, D., Faber, S. M., Burstein, D., Davies, R. L., Dressler, A., Terlevich, R., and Wegner, G. 1988, *Ap. J.*, **326**, 19.
 Nilson, P. 1973, *Uppsala General Catalogue of Galaxies* (Uppsala: Uppsala Obs. Ann.)
 Pierce, M. J., and Tully, R. B. 1988, *Ap. J.*, **330**, 579.
 Schneider, D. P., Gunn, J. E., and Hoessel, J. G. 1983, *Ap. J.*, **264**, 337.
 Teerikorpi, P. 1987, *Astr. Ap.*, **173**, 39.

J. A. WILLICK: Space Sciences Laboratory, University of California, Berkeley, CA 94720